Springer

KSME

Journal of Mechanical Science and Technology 26 (8) (2012) 2247~2257
www.springerlink.com/content/1738-494x
DOI 10.1007/s12206-012-0606-1

Three-dimensional computational fluid dynamic analysis of the conventional PEM fuel cell and investigation of prominent gas diffusion layers effect †

N. Ahmadi[1,*], S. Rezazadeh[2], I. Mirzaee[1] and N. Pourmahmoud[1]

[1]*Mechanical Engineering Department, Urmia University of Technology, Iran*
[2]*CFD Research center, Mechanical Engineering Department, Urmia University, Iran*

(Manuscript Received August 17, 2011; Revised March 9, 2012; Accepted March 25, 2012)

Abstract

A full three-dimensional, single phase computational fluid dynamics model of a proton exchange membrane fuel cell (PEMFC) with both the gas distribution flow channels and the membrane electrode assembly (MEA) has been developed. A single set of conservation equations which are valid for the flow channels, gas-diffusion electrodes, catalyst layers, and the membrane region are developed and numerically solved using a finite volume based computational fluid dynamics technique. In this research some parameters such as oxygen consumption, water production, velocity distribution, ohmic losses, liquid water activity and fuel cell performance for straight (base case) and prominent gas diffusion layers were investigated in more detail. The numerical simulations reveal that prominent gas diffusion layer improves the transport of the reactant gases through the porous layers; it is due to increase of the mentioned fuel cell efficiency, and prominent gas diffusion layers yield appreciably higher current density. Finally the numerical results of proposed CFD model (base case) are compared with the available experimental data that represent good agreement.

Keywords: PEM fuel cell; Geometrical configuration; GDL prominence; CFD; Fuel cell performance

1. Introduction

The proton exchange membrane fuel cell (PEMFC) using very thin polymer membrane as electrolyte has been considered as a promising candidate of future power sources, especially for transportation applications and residential power. This type of fuel cell has many important advantages such as high efficiency, clean, quiet, low temperature operation, capable of quick start-up, no liquid electrolyte and simple cell design. However, its performance and cost should be further optimized before this system becomes competitive with the traditional combustion power plants.

The most attractive choice among variety of fuel cell is polymer electrolyte membrane fuel cell (PEMFC). In PEMFC, there is a solid polymer electrolyte conducting protons between two platinum impregnated porous electrodes, the present electrodes are cast as thin films and bonded to the membrane. William T. Grubbs [1] originally performed the use of organic cation exchange membrane polymers in fuel cells in 1959. One of the popular electrolytes used in PEMFC is Nafion. Water produces as liquid instead of steam in a PEMFC. The first three-dimensional model was presented by Dutta et al. in 2000 [2] Berning, Djilali and Li et al. have also developed steady-state, three-dimensional, non-isothermal models for [3] proton exchange membrane fuel cell (PEMFC) have been extensively suggested for future power supply in the vehicles, by developing the power generation systems and electronically applications. Although researches and investigations in fuel cell systems have been developed a lot, but these systems and applications are still very expensive and complicated. So they are not commercialized. Complete fuel cell systems have been demonstrated for a number of transportation applications including public transit buses and passenger automobiles. One of the most important goals of recent development has been cost reduction and high volume manufacture for the catalyst, membranes, and bipolar plates. This issue will come off by ongoing research to increase power density, improve water management, operate at ambient conditions, tolerate reformed fuel, and extend stack life.

In recent years various research and experiments on PEMFCs, by various geometries have been developed. Two geometries with rectangular and trapezoidal channel configuration were simulated and the obtained results in a low cell voltage (which leads to high current densities in two geometries) compared. S. Rezazadeh et al. investigated the gas diffusion layer thickness effect on PEMFC performance [4, 5].

One of the main requirements of these cells is maintaining a

*Corresponding author. Tel.: +989143474974, Fax.: +984412773591
E-mail address: nima.ahmadi.eng@gmail.com
† Recommended by Associate Editor Yong-Tae Kim

high water content in the electrolyte to ensure high ionic conductivity. During the reactive mode of operation, water content in the cell, will be determined by the balance of water or its transport. Contributing factors to water transport are the water drag through the cell, back diffusion from the cathode, and the diffusion of any water in the fuel stream through the anode. Water transport is function of current and the characteristics of the membrane and the electrodes.

Water drag refers to the amount of water that pulled by osmotic action along with the proton direction. Water management has a noticeable impact on cell performance, because at high current densities mass transport issues associated with water formation and distribution limit cell output. Without proper water management, an imbalance will happen between water production and evaporation within the cell. As a negative effect, dilution of reactant gases by water vapor, flooding of the electrodes, and dehydration of the solid polymer membrane. If dehydration occurs, the adherence of the membrane to the electrode also will be adversely affected. As there is no free liquid electrolyte to form a conducting bridge so intrinsic contact between the electrodes and the electrolyte membrane is important. If water was exhausted more than produced, thus it is important to humidify the incoming anode gas. If there is too much humidification, however, the electrode floods, which causes problems with diffusing the gas to the electrode. A smaller current, larger reactant flow, lower humidity, higher temperature, or lower pressure will result in a water deficit. A higher current, smaller reactant flow, higher humidity, lower temperature, or higher pressure will lead to a water surplus. There have been attempts to use external wicking connected to the membrane to either drain or supply water by capillary action in order to control the water in the cell. The ionic conductivity of the electrolyte is higher when the membrane is fully saturated, and this offers a low resistance to current flow and increases efficiency. Operating temperature has a significant influence on PEMFC performance. If the temperature increases the internal resistance of the cell will decrease, mainly by downfall of the ohmic resistance of the electrolyte. In addition, mass transport limitations get reduced at higher temperatures. The overall result is an improvement in cell performance. Experimental data [6, 7] suggest a voltage gain in the range of 1.1 mV to 2.5 mV for each degree (^{o}C) of temperature increase. Improving cell performance by increasing in temperature, however, limited by the high vapor pressure of water in the ion exchange membrane. This is due to the membrane's susceptibility to dehydration and the subsequent loss of ionic conductivity. Operating pressure also influences cell performance. An increase in the oxygen pressure from 3 to 10.2 atmospheres produces an increase of 42 mV in the cell voltage at 215 mA/cm^2. According to the Nernst equation, by growing up the reversible cathode potential which is expected for this increase in oxygen pressure, is about 12 mV, which is considerably less than the measured value. Performance improvements due to increased pressure must be balanced against the energy required to pressurize the reactant gases.

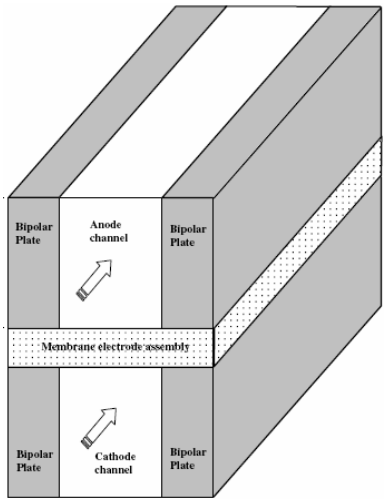

Fig. 1. Schematic of a single straight-channel of PEMFC.

The overall system must be optimized according to output, efficiency, cost, and size. Operating at pressure above ambient conditions would most likely be reserved for stationary power applications. Because of no material found by zero permeability, some researches and investigations have been done by mathematical and numerical modeling of fuel cell, which respect bipolar plates as another parts of PEMFC as gas diffusion layers. Gas diffusion layers are usually fabricated with carbon fiber or carbon cloth and functions to wick away liquid water, transport reactants of H_2 and O_2 and conduct electrons. Its thickness is normally between 200 and 300μm [8, 9]. Design of a flow channel is very complicated and difficult to optimize geometry, shape and size of flow fields like that the gas flow channels and bipolar plates since there are many parameters which affect the fuel cell operation such as different materials use in cathode and anode bipolar plates [9] channel/rib ratio [10], and channel path length [11] Catalyst layer which is the region where the membrane and the electrodes overlap and the H_2 oxidation or O_2 reduction reaction occur. It allows electron and ion conduction at the same time. There are other parameters, which affect cell performance such as operating temperature, pressure and humidification of the gas in the cell. It is necessary to understand these parameter and their effects on cell performance. For this reasons we understand it is a point to set up these design factors at optimum values in order to increase the PEMFC operation performance. In this model, major transport phenomena in PEMFC and the effects of prominent gas diffusion layers on cell performance and output cell voltage were studied. The modeling data for base case validate with experimental data.

2. Mathematical model

Fig. 1 shows a schematic of a single cell of a PEMFC. It is made of two porous electrodes, a polymer electrolyte membrane, two-catalyst layer and two-gas distributor plates. The membrane is sandwiched between the gas channels.

3. Model Assumptions

Present model includes some assumptions such as: All gases are assumed to be ideal gas mixture, GDLs and catalyst layers are homogeneous porous, flow is incompressible and laminar, because the pressure gradients and velocities are small and volume of liquid-phase water in the domain is negligible, so the flow field is single phase.

4. Governing equations

In this numerical simulation, a single domain model formation was used for the governing equations. These governing equations consist of mass conservation, momentum and species equations, which can be written as:

$$\left(\nabla.\rho \mathrm{u}\right)=0 \tag{1}$$

$$\frac{1}{\left(\varepsilon^{eff}\right)^2}\nabla.\left(\rho \mathrm{uu}\right)=-\nabla P+\nabla.\left(\mu\nabla \mathrm{u}\right)+S_u \tag{2}$$

$$\nabla.\left(\mathrm{u}C_K\right)=\nabla.\left(D_K^{eff}\nabla C_K\right)+S_K \tag{3}$$

$$\nabla.\left(\kappa_e^{eff}\nabla\Phi_e\right)+S_\Phi=0 \tag{4}$$

where ρ is the density of gas mixture in Eq. (1). According to model assumption, mass source and sink term neglected. ε is the effective porosity inside porous mediums, and μ is the viscosity of the gas mixture in the momentum equation is shown as Eq. (2) The momentum source term, S_u, is used to describe Darcy's drag for flow through porous gas diffusion layers and catalyst layers [12] As:

$$S_u=-\frac{\mu}{K}\mathrm{u}\,. \tag{5}$$

K is the gas permeability inside porous mediums. D_K^{eff} In the species equation as shown in Eq. (3), is the effective diffusion coefficient of species k (e.g. hydrogen, oxygen, nitrogen and water vapor) and is defined to describe the effects of porosity in the porous gas diffusion and catalyst layers by the Bruggeman [13] correlation as:

$$D_K^{eff}=\left(\varepsilon^{eff}\right)^{1.5}D_K\,. \tag{6}$$

Additionally, diffusion coefficient is function of temperature and pressure [14] by the next equation:

$$D_K=D^{\circ}{}_K\left(\frac{T}{T_\circ}\right)^{\frac{3}{2}}\left(\frac{P_\circ}{P}\right). \tag{7}$$

Transport properties for species are given in Table 1.

The charge conservation equation is shown as Eq. (4) and κ_e is the ionic conductivity in the ion metric phase and has been incorporated by Springer et al. [15] as:

Table 1. Transport properties [14].

Property	Value
H_2 Diffusivity in the gas channel, D^0_{H2}	1.10×10^{-04} m^2/s
O_2 Diffusivity in the gas channel, D^0_{o2}	3.20×10^{-05} m^2/s
H_2O Diffusivity in the gas channel, D^0_{H2o}	7.35×10^{-05} m^2/s
H_2 Diffusivity in the membrane, D^{mem}_{H2}	2.59×10^{-10} m^2/s
O_2 Diffusivity in the membrane, D^{mem}_{o2}	1.22×10^{-10} m^2/s

Table 2. Source/sink term for momentum, species and charge conservation equations for individual regions.

	Momentum	Species	Charge
Flow channels	$S_u=0$	$S_K=0$	$S_\Phi=0$
Bipolar plates	$S_u=-\frac{\mu}{K}\mathrm{u}$	$S_K=0$	$S_\Phi=0$
GDLs	$S_u=-\frac{\mu}{K}\mathrm{u}$	$S_K=0$	$S_\Phi=0$
Catalyst layers	$S_u=0$	$S_K=-\nabla.\left(\frac{n_d}{F}I\right)-\frac{S_K j}{nF}$	$S_\Phi=j$
Membrane	$S_u=0$	$S_K=-\nabla.\left(\frac{n_d}{F}I\right)$	$S_\Phi=0$

$$\kappa_e=exp\left[1268\left(\frac{1}{303}-\frac{1}{T}\right)\right]\times(0.005139\lambda-0.00326)\,. \tag{8}$$

Moreover, in recent equation, λ is defined as the number of water molecules per sulfonate group inside the membrane. The water content can be assumed function of water activity, a is defined according to experimental data [16]:

$$\lambda=0.3+6a\left[1-\tanh\left(a-0.5\right)\right]+3.9\sqrt{a}\left[1+\tanh\left(\frac{a-0.89}{0.23}\right)\right]. \tag{9}$$

Water activity, a is defined by:

$$a=\frac{C_w RT}{P_w^{sat}}\,. \tag{10}$$

The proton conductivity in the catalyst layers by introducing the Bruggeman correlation [17] can be given by:

$$\kappa_e^{eff}=\varepsilon_m^{1.5}\kappa_e\,. \tag{11}$$

In recent equation ε_m is the volume fraction of the membrane-phase in the catalyst layer.

The source and sink term in Eqs. (3) and (4) are presented in Table 2.

Local current density in the membrane can be calculated by:

$$I = -\kappa_e \nabla \Phi_e \,. \tag{12}$$

Then the average current density is calculated as follows:

$$I_{ave} = \frac{1}{A} \int_{A_{mem}} IdA \tag{13}$$

where A is the active area over the MEA.

5. Water transport

Water molecules in PEM fuel cell are transported via electro-osmotic drag due to the properties of polymer electrolyte membrane in addition to the molecular diffusion. H^+ protons transport water molecules through the polymer electrolyte membrane and this transport phenomenon is called electro-osmotic drag. In addition to the molecular diffusion and electro-osmotic drag, water vapor is also produced in the catalyst layers due to the oxygen reduction reaction.

Water transport through the polymer electrolyte membrane is defined by:

$$\nabla.\left(D_{H_2o}^{mem} \nabla C_{H_2o}^{mem}\right) - \nabla.\left(\frac{n_d}{F} \boldsymbol{i}\right) = 0 \tag{14}$$

where n_d and are $D_{H_2o}^{mem}$ defined as the water drag coefficient from anode to cathode and the diffusion coefficient of water in the membrane phase, respectively.

The number of water molecules transported by each hydrogen proton H^+ is called the water drag coefficient. It can be determined from the following equation [16]:

$$n_d = \begin{cases} 1 & \lambda < 9 \\ 0.117\lambda - 0.0544 & \lambda \geq 9 \,. \end{cases} \tag{15}$$

The diffusion coefficient of water in the polymer membrane is dependent on the water content of the membrane and is obtained by the following fits of the experimental expression [18]:

$$D_w^{mem} = \begin{cases} 3.1\times10^{-7}\,\lambda(e^{0.28\lambda}-1)e^{\left(\frac{-2346}{r}\right)} & 0<\lambda\leq 3 \\ 4.17\times10^{-1}\,\lambda(1+161e^{-\lambda})e^{\left(\frac{-2346}{r}\right)} & otherwise \,. \end{cases} \tag{16}$$

The terms are therefore related to the transfer current through the solid conductive materials and the membrane. The transfer currents or source terms are non-zero only inside the catalyst layers. The transfer current at anode and cathode can be described by Tafel equations as follows:

$$R_{an} = j_{an}^{ref}\left(\frac{[H_2]}{[H_2]_{ref}}\right)^{\gamma an}\left(e^{\alpha_{am}F\eta_{an}/RT} - e^{-\alpha_{cat}F\eta^{an}/RT}\right) \tag{17}$$

$$R_{cat} = j_{an}^{ref}\left(\frac{[O_2]}{[O_2]_{ref}}\right)^{\gamma cat}\left(-e^{\alpha_{am}F\eta_{cat}/RT} + e^{-\alpha_{cat}F\eta\ cat/RT}\right). \tag{18}$$

According to the Tafel equation, the current densities in the anode and cathode catalysts can be expressed by the exchange current density, reactant concentration, temperature and over-potentials according to the Tafel equations. Where, the surface over potential is defined as the difference between proton potential and electron potential.

$$\eta_{an} = \varphi_{sol} - \varphi_{mem} \tag{19}$$

$$\eta_{cat} = \phi_{sol} - \phi_{mem} - V_{oc} \tag{20}$$

The open circuit potential at the anode is assumed to be zero, while the open circuit potential at the cathode becomes a function of a temperature as:

$$V_{oc} = 0.0025T + 0.2329 \,. \tag{21}$$

The protonic conductivity of membrane is dependent on water content, where σ_m is the ionic conductivity in the ionomeric phase and has been correlated by Springer et al. [19]:

$$\sigma_m = (0.005139\lambda - 0.00326)\exp\left[1268\left(\frac{1}{303} - \frac{1}{\mathrm{T}}\right)\right]. \tag{22}$$

Energy equation given by Eq. (23):

$$\nabla.(\rho \mathbf{u}\mathrm{T}) = \nabla.(\lambda_{\mathrm{eff}}\nabla\mathrm{T}) + \mathrm{s_T} \tag{23}$$

where, λ_{eff} is the effective thermal conductivity, and the source term of the energy equation, S_T, is defined with the following equation:

$$S_T = I^2 R_{ohm} + h_{reaction} + \eta_a i_a + \eta_c i_c \,. \tag{24}$$

In this equation, R_{ohm} , is the ohmic resistance of the membrane, $h_{reaction}$, is the heat generated thorough the chemical reactions, η_a and η_c, are the anode and cathode overpotentials, which are calculated as:

$$R_{ohm} = \frac{t_m}{\sigma_e} \,. \tag{25}$$

Here, t_m is the membrane thickness.

$$\eta_a = \frac{RT}{\alpha_a F}\ln\left[\frac{IP}{j_{0_a} P_{0_{H_2}}}\right] \tag{26}$$

$$\eta_C = \frac{RT}{\alpha_c F}\ln\left[\frac{IP}{j_{0_c} P_{0_{O_2}}}\right] \tag{27}$$

where α_a and, α_c are the anode and cathode transfer coefficients, $P_{0_{O_2}}$ is the partial pressure of hydrogen and oxygen, and, j_0 is the reference exchange current density.

The fuel and oxidant fuel rate **u** is given by following equations:

$$\mathbf{u}_{in,a} = \frac{\xi_a I_{ref} A_{mem}}{2C_{H_2,in} F A_{ch}}$$
$$\mathbf{u}_{in,c} = \frac{\xi_c I_{ref} A_{mem}}{4C_{O_2,in} F A_{ch}}. \quad (28)$$

In the present equation, I_{ref} and ξ are the reference current density and stoichiometric ratio, respectively. ξ is defined as the ratio between the amount supplied and the amount required of the fuel based on the reference current density. The species concentrations of flow inlets are assigned by the humidification conditions of both the anode and cathode inlets.

6. Boundary condition

Eqs. (1)-(4) form the complete set of governing equations for the traditional mathematical model. Boundary conditions are dispensed at the external boundaries. Constant mass flow rate at the channel inlet and constant pressure condition at the channel outlet, the no-flux conditions are executed for mass, momentum, species and potential conservation equations at all boundaries except for inlets and outlets of the anode and cathode flow channels.

7. Results and discussion

7.1 Model validation

A series of simulation were carried out on the model from low to high operating current densities. In order to evaluate the validity of the model, numerical simulation results (for conventional model) compared with the experimental data presented by Wang et al. [20], as shown in Fig. 2, which there is a favorable agreement between them. The power density curve for the model is illustrated too. As we know, there is a relation between voltage, current density and the power of the fuel cell as P =V*I. Fuel cell operating condition and geometric parameters are shown in Table 3. It is used fully humidified inlet condition for anode and cathode. The transfer current at anode and cathode can be described by Tafel equations.

At the first some of the important diagrams for conventional model are presented; such as oxygen mass fraction, water mass fraction and current flux density at the cathode GDL–cathode catalyst interface. They can give important details about the flow patterns of fuel cell.

According to Fig. 3 oxygen mass fraction is high at the entrance region. It decreases along the fuel cell due to oxygen consumption. This fact leads to water formation. On the other word, water formation is related to electrochemical reaction, which occurs at the cathode catalyst layer. Obviously in this reaction oxygen is being consumed. On the other hand, water can be transported from anode side by electro-osmotic drag coincidently. It results in water mass fraction increase along the fuel cell.

In addition, it can be anticipated that the mass fraction of oxygen and water will be decreased and increased respectively, by increasing of cell voltage due to increasing the electrochemical reaction rate.

Table 3. Geometrical parameters and operating conditions [20].

Parameter	Value
Gas channel length	7.0×10^{-2} m
Gas channel width and depth	1.0×10^{-3} m
Bipolar plate width	5.0×10^{-4} m
Gas diffusion layer thickness	3.0×10^{-4} m
Catalyst layer thickness	1.29×10^{-5} m
Membrane thickness	1.08×10^{-4} m
Cell temperature	70°C
Anode pressure	3 atm
Cathode pressure	3 atm

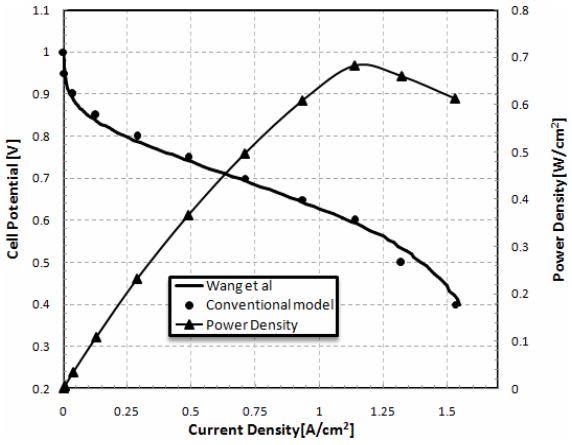

Fig. 2. Measured and predicted cell polarization curves density.

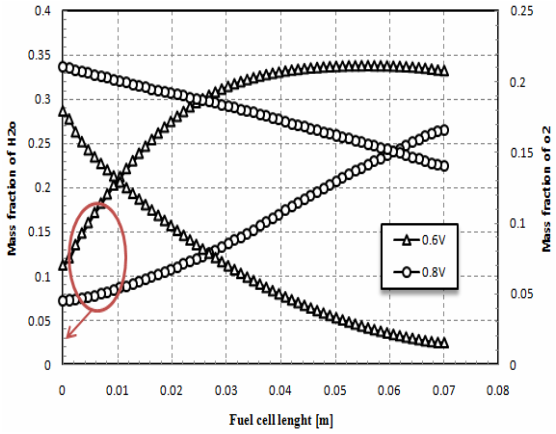

Fig. 3. Comparison water and oxygen mass fraction at the interface of cathode GDL and cathode catalyst layer for two different cell voltages, along the cell.

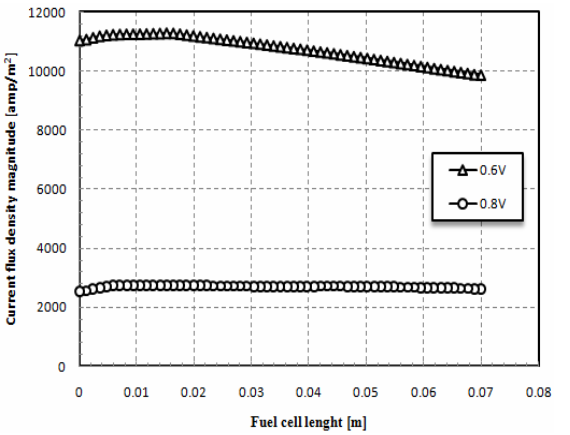

Fig. 4. Comparison current flux density at the Interface of cathode GDL and cathode catalyst layer for two different cell voltages, along the cell.

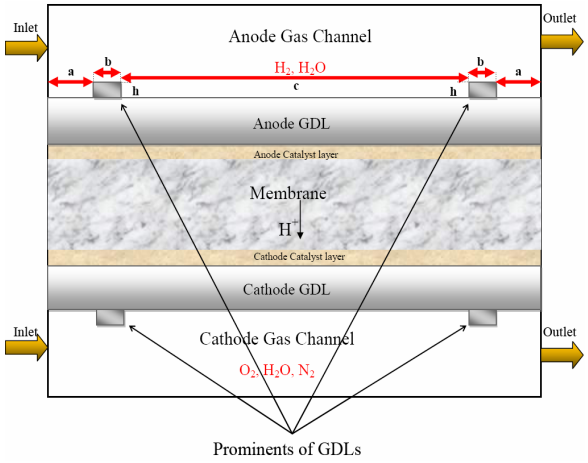

Fig. 5. Side view schematic of case with prominent GDLs.

The current density on the catalyst layer is shown in Fig .4. At the inlet region it reaches to its highest value and decreases along the cell. The highest value of current flux density at the inlet region is probably because of the high concentration of hydrogen and oxygen and high electro-osmotic mass flux at the inlet region.

In present study, also the effect of prominent gas diffusion layers (shown in Fig. 5) on cell performance has been studied and compared with conventional model (base case).

Geometrical properties of proposed model have been given in Table 4.

Fig. 6 shows side view schematic of conventional model (base case). Figs. 7 and 8 compare polarization and power density curves of two numerical cases, respectively.

Numerical results show that case with prominent GDLs produces more current density than conventional model at the same cell voltage. It is clear that the case with prominent GDLs yields a notable increase in velocity. Prominences of GDLs increase the velocity by decreasing the cross sectional area of gas flow at gas channels.

Table 4. Geometrical specification of case with prominent GDLs.

Symbol	Value
a	15 mm
b	5 mm
c	30 mm
h	0.25 mm

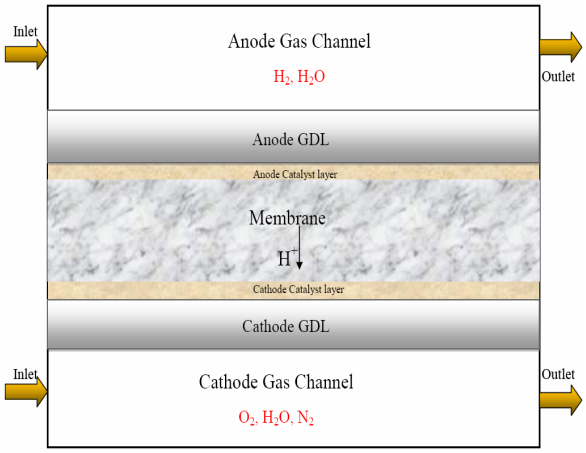

Fig. 6. Side view schematic of base case.

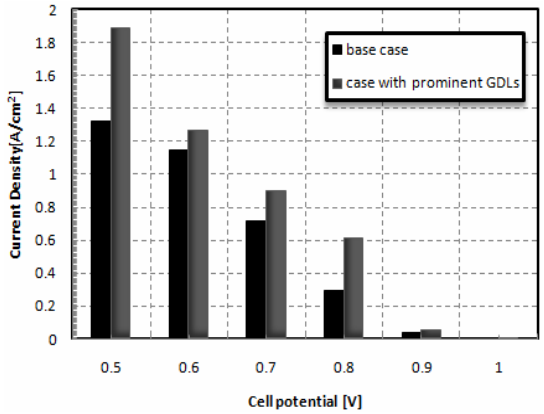

Fig. 7. Comparison polarization curves of two numerical models.

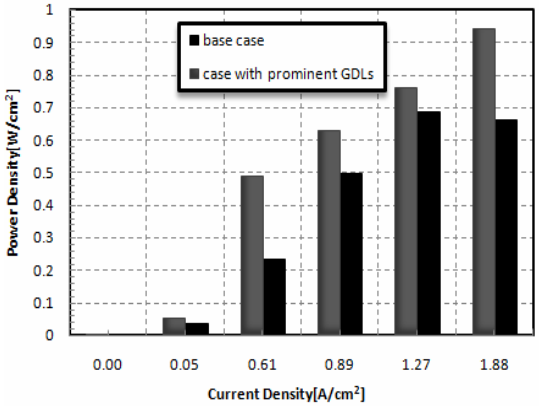

Fig. 8. Comparison power density curve of two numerical models.

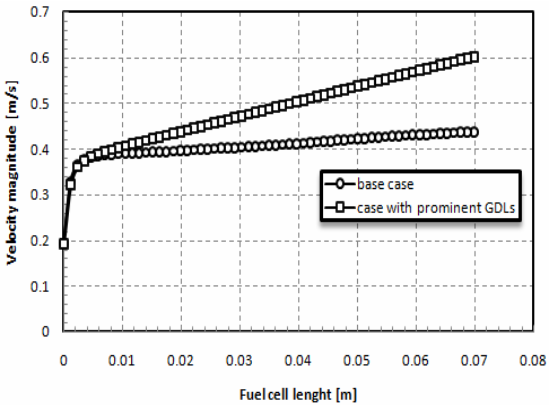

Fig. 9. Comparison velocity magnitude of two numerical cases at cathode gas flow channel along the fuel cell.

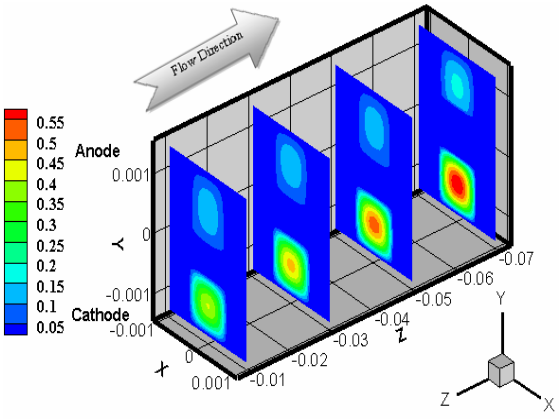

Fig. 11. Velocity magnitude for case with prominent GDLs.

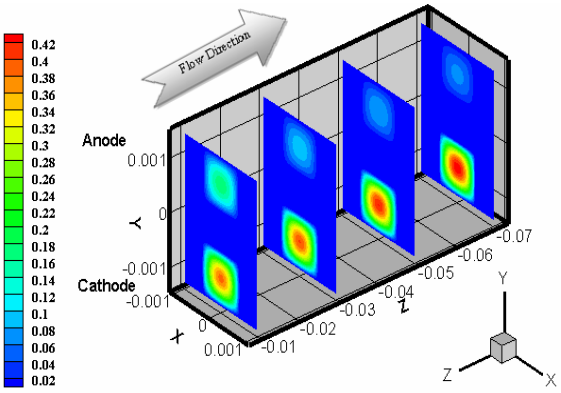

Fig. 10. Velocity magnitude for base case.

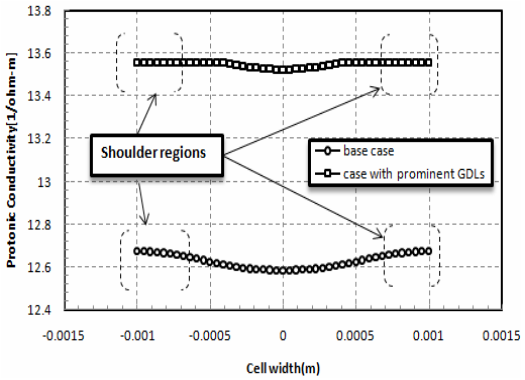

Fig. 12. Comparison protonic conductivity at the Interface of membrane and cathode catalyst layer for two numerical model at entry region ($L/L_0 = 0.1428$) at same voltage (0.8 volt).

Increasing in velocity magnitude supplies the reactant gases to the catalyst layers. Thus the efficiency of catalytic reaction enhances, therefore PEMFC performance improves. Fig. 9 illustrates the comparison velocity distribution of at cathode gas channel.

On the other hand, the interface of GDLs and reactant gases grows up and subsequently reactants diffuse to catalyst layers better than conventional model.

Fig. 10 and Fig. 11 show the contours of velocity distribution for two cases at same cell voltage (at 0.8 volt) and confirm the mentioned details.

Also Prominences of GDLs improve the flow of the reaction hence reduces the membrane drawing effect.

Thus the performance of fuel cell especially at higher current density region improves.

The comparison of protonic conductivity at membrane and cathode catalyst layer interface for entry region is shown in Fig. 12. The prominence of GDLs increases reactant surface at GDLs, therefore ability of membrane in protonic conduction increases. The protonic conductivity of proposed model is higher than conventional model. Protonic conductivity depends on the water content and temperature. It is higher in shoulder area and lower in channel area due to higher thermal conductivity of bipolar plates leads to lower temperature in shoulder region than the channel area. Ohmic resistance calculated by Eq. (25). Ohmic loss is achieved form multiplying the ohmic resistance and current density. Thus, ohmic loss is directly related to the membrane thickness, tm, and local current density, I, and inversely related to the membrane conductivity, σ_e. Fig. 13 shows the ohmic loss at the membrane-cathode catalyst interface for entry region.

Fig. 14 illustrates the distribution of oxygen mass fraction at membrane-cathode catalyst interface, for two different cases at the entry region of fuel cell. Therefore in case with prominent GDLs the performance of the cell is higher than the result of conventional model, especially at higher current density region. This fact is because of electrochemical reaction rate improvement (which mentioned before).

Lack of oxygen at the cell shoulder regions causes to higher mass fraction losses.

For downstream region of channel high mass fraction losses becomes worse due to diminution of the reactant with moving downstream which shown in Fig. 15. The contour of oxygen mass fraction at interface of membrane and cathode catalyst layer is shown in Fig. 16. This figure shows that oxygen mass fraction decreases gradually along the flow channel due to the

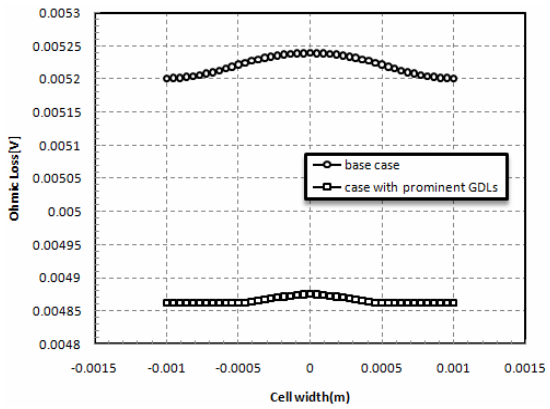

Fig. 13. Comparison ohmic loss at the Interface of membrane and cathode catalyst layer for two different numerical model at entry region ($L/L_0 = 0.1428$) at same voltage (0.8 volt).

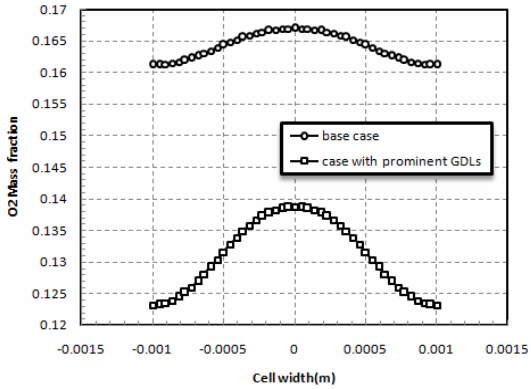

Fig. 14. Comparison oxygen mass fraction at the Interface of membrane and cathode catalyst layer for two numerical model at entry region ($L/L_0 = 0.1428$) at same voltage (0.8 volt).

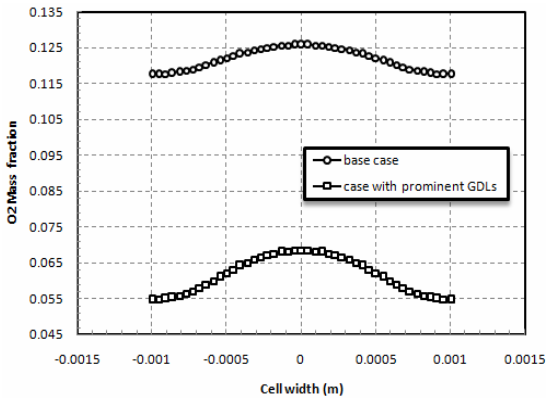

Fig. 15. Comparison oxygen mass fraction at the Interface of membrane and cathode catalyst layer for two numerical model at exit region ($L/L_0 = 0.8571$) at same voltage (0.8 volt).

consumption of oxygen at cathode catalyst layer.

In this layer, the concentration of oxygen is balanced by consuming the oxygen and the amount of oxygen that diffuses

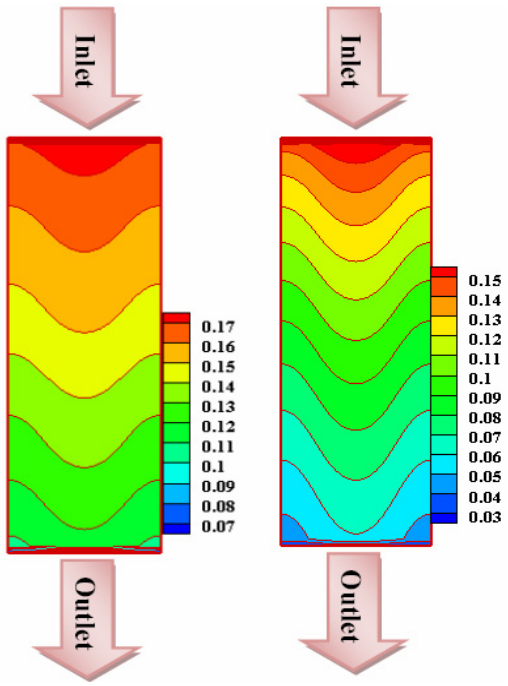

Fig. 16. Oxygen mass fraction at the Interface of membrane and cathode catalyst layer for base case (left) and case with prominent GDLs (right) at same voltage (0.8 volt).

towards the catalyst layer, driven by the concentration gradient. The lower diffusivity of the oxygen along the flow with the low concentration of oxygen in ambient air results in noticeable oxygen diminution along the fuel cell.

Hydrogen at the anode side provides a proton, releasing an electron in the process that must pass through an external circuit to reach the cathode. The proton, which remains solvated with a certain number of water molecules, diffuses through the membrane to the cathode to react with oxygen and the returning electron. Water successively produced at the cathode.

Comparison of water mass fraction at the cathode side is shown in Figs. 17 and 18, respectively for entry and exit region of cell, for two cases.

Water concentration at the membrane and cathode catalyst layer interface, increases along the flow channel. Increasing of water concentration, associates with the phenomenon that the water composes by electrochemical reaction along the channel and transports from anode side by electro-osmotic drag coincidently. As it is clear from Fig. 19 the mass fraction of water for conventional model (base case) is lower than that in the proposed model.

Water activity depends on mass fraction of water in both anode and cathode sides. Therefore, at cathode side mass fraction of water increases along the flow channel hence water activity increases along the cathode flow channel.

Figs. 20 and 21 compare water activity for two cases at entry and exit regions, respectively. It is observed that the case with prominent GDLs has higher water activity along the cell. Figs. 22 and 23 confirm this fact.

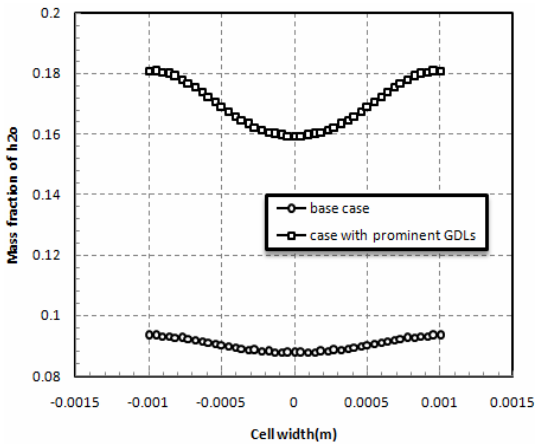

Fig. 17. Comparison water mass fraction at the Interface of membrane and cathode catalyst layer for two numerical model at entry region (L/L_0 = 0.1428) at same voltage (0.8 volt).

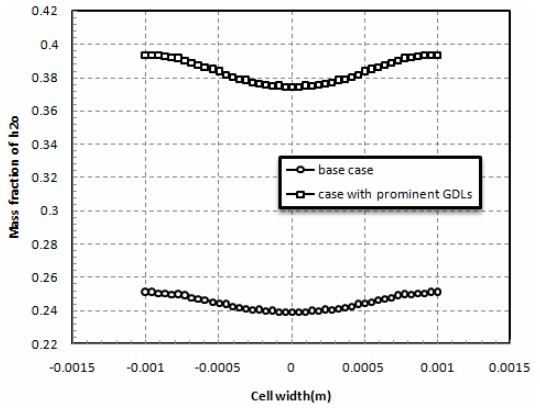

Fig. 18. Comparison water mass fraction at the Interface of membrane and cathode catalyst layer for two numerical model at exit region (L/L_0 = 0.8571) at same voltage (0.8 volt).

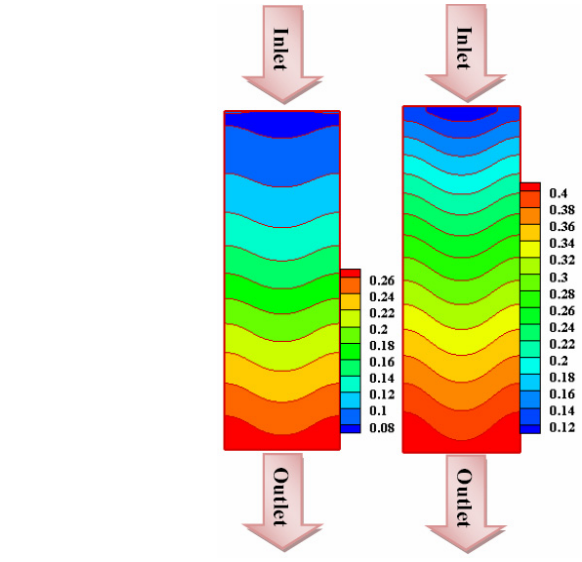

Fig. 19. Water mass fraction at the Interface of membrane and cathode catalyst layer for base case (left) and case with prominent GDLs (right) at same voltage (0.8 volt).

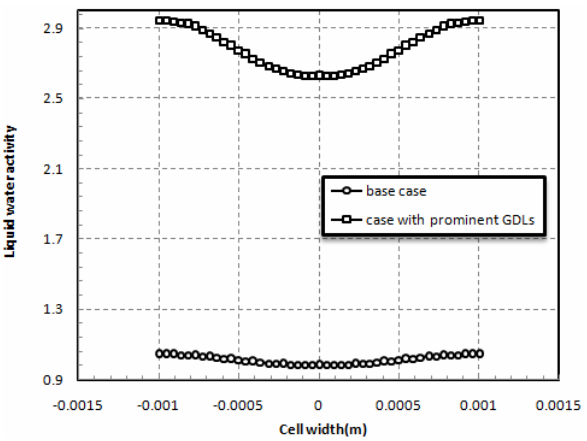

Fig. 20. Comparison liquid water activity at the Interface of membrane and cathode catalyst layer for two numerical model at entry region (L/L_0 = 0.1428) at same voltage (0.8 volt).

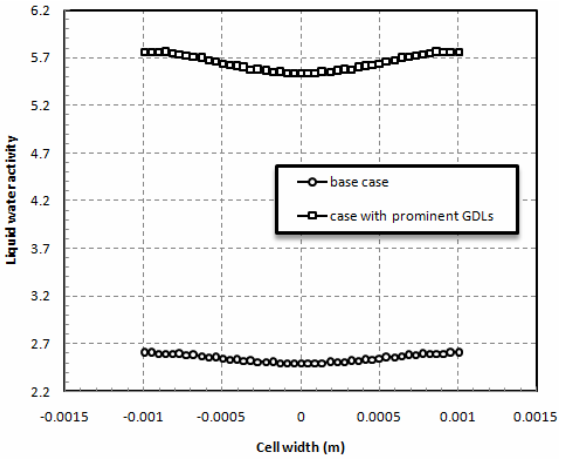

Fig. 21. Comparison liquid water activity at the Interface of membrane and cathode catalyst layer for two numerical model at exit region (L/L_0 = 0.8571) at same voltage (0.8 volt).

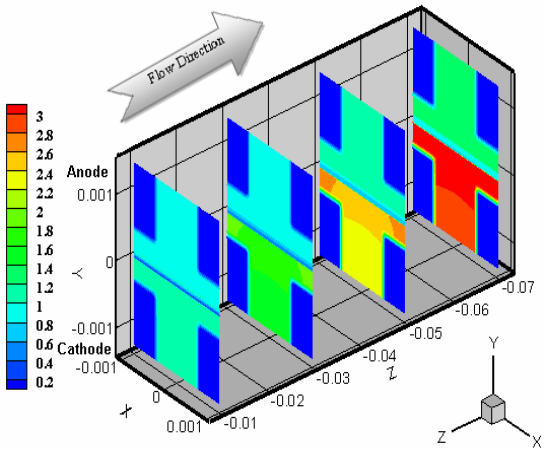

Fig. 22. Liquid water activity for base case (at 0.8 volt).

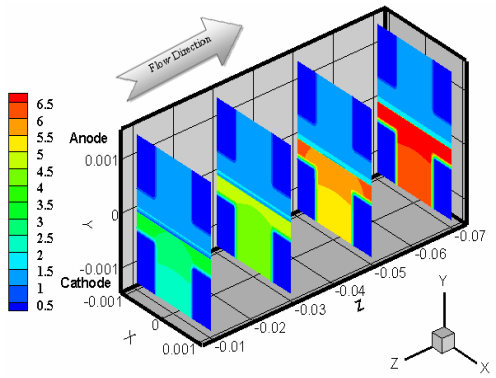

Fig. 23. Liquid water activity for case with prominent GDLs (at 0.8 volt).

8. Conclusions

In this article a three-dimensional computational fluid dynamics model of a Proton Exchange Membrane Fuel Cell (PEMFC) with straight flow channels has been simulated. In the present research a new geometry for PEM fuel cells consist of prominent gas diffusion layers has been studied. In this work the prominences of GDLs have been reposed at entry and exit region of gas flow channel for both the anode and cathode sides. Comparison the results of this new proposed numerical model, such as polarization and power density curves, velocity distribution and species mass fractions with conventional model results (the cell with no prominences) shows that new model can improve the fuel cell performance. It is due to improvement of the gas flow along the channel which supplies the reactant gases to the catalyst layers. Also the membrane drawing effect reduction is one of the other results of gas flow improvement in the flow channels, thus the efficiency of catalytic reaction increases. Therefore the performance of PEMFC enhances and it can be obtained that using these kinds of GDLs, in PEMFCs can be useful. Finally, the obtained numerical results for base model showed good agreement with the experimental data.

Nomenclature

a : Water activity
C : Molar concentration (mol/m^3)
D : Mass diffusion coefficient (m^2/s)
F : Faraday constant (C/mol)
I : Local current density (A/m^2)
J : Exchange current density (A/m^2)
K : Permeability (m^2)
M : Molecular weight (kg/mol)
n_d : Electro-osmotic drag coefficient
P : Pressure (Pa)
R : Universal gas constant (J/mol-K)
T : Temperature (K)
t : Thickness
$\vec{u}$: Velocity vector
V_{cell} : Cell voltage
V_{oc} : Open-circuit voltage
W : Width
X : Mole fraction

Greek letters

α : Water transfer coefficient
ε^{eff} : Effective porosity
ρ : Density (kg/m^3)
ϕ_e : Electrolyte phase potential (v)
μ : Viscosity (kg/m-s)
σ_e : Membrane conductivity (1/ohm-m)
λ : Water content in the membrane
ζ : Stoichiometric ratio
η : Over potential (v)
λ_{eff} : Effective thermal conductivity (w/m-k)

Subscripts and superscripts

a : Anode
c : Cathode
ch : Channel
k : Chemical species
m : Membrane
MEA : Membrane electrolyte assembly
ref : Reference value
sat : Saturated
w : Water

References

[1] W. T. Grubb, Proceedings of the *11th annual battery research and development conference*, *PSC Publications Committee*, Red Bank, NJ, p. 5, 1957; U.S. Patent No. 2,913,511 (1959).
[2] S. Dutta, S. Shimpalee and J. W. Van Zee, Three-dimensional numerical simulation of straight channel PEM fuel cells, *Journal of Applied Electrochemistry*, 30 (2000) 135-146.
[3] V. Gurau, H. Liu and S. Kakac, Two-dimensional model for proton exchange membrane fuel cells, *AICHE Journal*, 44 (11) (1998) 2410-2422.
[4] S. Majidifar, I. Mirzaei, S. Rezazadeh, P. Mohajeri and H. Oryani, Effect of gas channel geometry on performance of pem fuel cells, *Australian Journal of Basic and Applied Sciences*, 5 (5) (2011) 943-954.
[5] N. Pourmahmoud, S. Rezazadeh, I. Mirzaee and V. heidarpoor, Three-dimensional numerical analysis of proton exchange membrane fuel cell, *Journal of Mechanical Science and Technology (JMST),* 25 (10) (2011) 2665-2673.
[6] Fuel cell handbook EG&G services, Parsons, Inc.Science Applications International Corporation.
[7] J. C. Amphlett et al., The operation of a solid polymer fuel cell: a parametric model, *Royal Military College of Canada.*
[8] C. S. Lee, C. H. Yun and B. M. Kim, S. C. Jang and S. C. Yi, *J. ceramic processing research,* 6 (2) (2005) 188-195.
[9] A. Kumar and R. G. Reddy, *J. power sources, 114* (2003) 54-62.
[10] S. Shimpalee and J. W. Van Zee, Int. *J. Hydrog. Energy,* 32

(7) (2007) 842-856.
[11] S. Shimpalee, S. Greenway and J. W. Van Zee, *J. power sources,* 160 (2006) 398-406.
[12] V. Garau, H. Liu and S. Kakac, *AIChE J*., 44 (11) (1998) 2410-2422.
[13] R. E. Meredith and C. W. Tobias, *Advances in electrochemistry and electrochemical engineering 2* (C.W. Tobias, ed., Interscience Publishers, New York, 1960).
[14] R. B. Bird, W. E. Stewart and E. N. Lightfoot, *Transport phenomena* (John Wiley & Sons, Inc, 1960).
[15] T. E. Springer, T. A. Zawodzinski and S. Gottesfeld, *J. electrochem. Soc.*, 138 (1991) 2334-2342.
[16] A. A. Kuklikovsky, *J. electrochem. Soc.,* 150 (11) (2003) A1432-A1439.
[17] R. E. Meredith and C. W. Tobias, *Advances in electrochemistry and electrochemical engineering 2*, (C.W. Tobias, ed., Interscience Publishers, New York, 1960).
[18] S. W. Yeo and A. Eisenberg, *J. Appl. Polym. Sci.,* 21 (1997) 875.
[19] T. E. Springer, T. A. Zawodinski and S. Gottesfeld, *J. electrochem. Soc.*, 136, 2334 (1991).
[20] L. Wang, A. Husar, T. Zhou, and H. Liu, *Int. J. Hydrog. Energy,* 28 (11) (2003) 1263-1272.

Nima Ahmadi was born in Urmia in 1984. He passed entrance exam of Technical University of Urmia in mechanical course in 2002. After finishing B.S, he was accepted in master degree of the same course at Urmia University of Technology (energy conversion tendency). And now he is in the last year of his M.Sc studying.

Sajad Rezazadeh was born in Urmia in 1984. He passed entrance exam of Technical University of Urmia in mechanical course in 2002. Immediately after finishing B.S, He was accepted in master degree of the same course (energy conversion tendency). He finished his M.S with a thesis about computational fluid dynamics modeling of proton exchange membrane fuel cell. During that year he was accepted in Ph.D and now he is in his second year of his Ph.D. During this nearly 8 years, he has presented several articles in internal and international seminars about main mechanical topics such as fuel cells and heat exchangers.

Iraj Mirzaee was born in 1960 in Ahar city in Iran. He received BS degree in Mechanical Engineering in Mashhad University in 1986. He started Msc. degree in mechanical engineering (energy conversion field) in Esfehan University in Iran and finally he re received his Ph.D in mechanical engineering (energy conversion field) in 1997 at the Bath University in England. He is an associated professor in the Mechanical Engineering Department at Faculty of Engineering of Urmia University. His professional interests are in the field of CFD, turbulent, fluid flow, energy conversion problems and turbine gas.

Nader Pourmahmoud was born in 1969 in Oshnavieh city in Iran. He received BS degree in Mechanical Engineering in Shiraz University in 1992. After achieving some of practical engineering projects till 1997 he started Msc. degree in mechanical engineering (energy conversion field) in Tarbiat Modarres University in Tehran and finally he received his Ph.D in mechanical engineering (energy conversion field) in 2003 at the same university in Iran. He is an assistance professor in the Mechanical Engineering Department at Faculty of Engineering of Urmia University. His professional interests are in the field of CFD of turbulent fluid flow, energy conversion problems and especially in fabricating of specific Vortex Tube.